IEEE Access
Multidisciplinary | Rapid Review | Open Access Journal

Received 28 April 2022, accepted 12 June 2022, date of publication 23 June 2022, date of current version 5 July 2022.

Digital Object Identifier 10.1109/ACCESS.2022.3185780

Supplemental Control for System Frequency Support of DFIG-Based Wind Turbines

MOHAMED ABDEEN[1], MUHAMMAD SAYYED[1], JOSÉ LUIS DOMÍNGUEZ-GARCÍA[2], (Senior Member, IEEE), AND SALAH KAMEL[3]

[1]Department of Electrical Engineering, Faculty of Engineering, Al-Azhar University, Cairo 11865, Egypt
[2]IREC Catalonia Institute for Energy Research, Sant Adrià de Besòs, 08930 Barcelona, Spain
[3]Department of Electrical Engineering, Faculty of Engineering, Aswan University, Aswan 81542, Egypt

Corresponding author: Salah Kamel (skamel@aswu.edu.eg)

This work was supported in part by the European Union's Horizon 2020 Research and Innovation Programme through the Marie Skłodowska-Curie Grant under Agreement 801342 (Tecniospring INDUSTRY), and in part by the Government of Catalonia's Agency for Business Competitiveness (ACCIÓ).

ABSTRACT Due to the shortage and environmental pollution of fossil fuel sources, conventional generating units are substituted with renewable energy sources. Thus, the total inertia decreases while the rate of change of frequency (ROCOF) increases, affecting the system frequency and stability. In this paper, a supplementary control, washout filter, is added to the primary frequency control of a doubly-fed induction generator (DFIG)- based wind turbine for better frequency regulation. In order to achieve the best performance (lowest frequency deviation with keeping the system stable), a new optimization technique called Mayfly Algorithm (MA) is used to find the optimum values of the washout filter's parameters. Compared with the traditional method, a great improvement has been presented in the system frequency response under different load perturbations. Also, the results show that the washout filter's parameters have an adverse impact on the frequency response and system stability if they aren't determined accurately. MATLAB/SIMULINK program is used to test the performance of the improved method under different scenarios.

INDEX TERMS Primary frequency control, DFIG wind turbine, washout filter, mayfly algorithm (MA), stability.

I. INTRODUCTION

Due to the daily technological applications development, more generated power is required to fulfill the increasing consumer demand. The lack of fossil fuel sources and their significant impact on the atmosphere prompted the world to shift to renewable energy sources (RESs) such as wind energy, solar energy, geothermal energy, etc., [1], [2]. Since the traditional generating units such as synchronous generators have high inertia as well as their directly connecting to the grid, a part of the kinetic energy stored in the rotor is released when the load is increased, leading to a smaller rate of change of frequency (ROCOF). Thus, the system frequency remains within the acceptable range. On the other hand, since the RESs have low inertia, a higher ROCOF occurs with changing the load. Thus, the system frequency is out of the acceptable range. With the high penetration of RESs in the power system, the number of the traditional generating units decreases. Consequently, the overall system inertia reduces, affecting the frequency stability with changing the load, and may even lead to a blackout [1]. Among the RESs, wind energy is the most prevalent. A doubly-fed induction generator (DFIG) is the most commonly used among the wind turbine technologies as it provides a safe operation within a wide range of wind speeds and can control the flow of both active and reactive powers towards and from the grid [3]. As its rotating mass is decoupled from the grid by a power electronic converter, DFIG can't contribute additional power using the stored kinetic energy in their rotating masses naturally [1]. In [4], a supplementary control loop was added to a DFIG controller for improving the system frequency. The supplementary control comprises a derivative block, a first-order filter block, and a gain block (inertia constant). The rotor speed was used as an input signal to the

The associate editor coordinating the review of this manuscript and approving it for publication was Ruisheng Diao.

This work is licensed under a Creative Commons Attribution 4.0 License. For more information, see https://creativecommons.org/licenses/by/4.0/

supplementary control. The output of this control was applied to the DFIG controller. The results proved the effectiveness of the proposed method for enhancing the system frequency. In [5], a non-standard inertial response method was proposed to support the system frequency, where the inertia constant was estimated according to the rotor speed. Compared to the traditional method (ideal inertial response), a shorter recovery period and less frequency deviation have been achieved. In [6], a supplemental control loop was presented to the DFIG controller. In this method, the difference between the measured and reference frequencies was applied to the drop control. Then, the sum of the output drop control and the load active power is the reference active power.

In [7] and [8], an additional system, a flywheel-based storage system, was inserted into the wind power plant to fulfill the power reserve requirements set by the network operator. This method can operate above and under-rated wind speeds. However, this method is costly. A variable droop control gain was introduced in [9] to reduce the frequency deviation under different system disturbances. The droop control gain is a function of the rotor speed. Compared to the traditional method (constant droop control gain), the proposed method achieved better performance. In [10], a primary frequency control support scheme of a DFIG was presented to enhance the settling frequency following an event. However, this method requires a monitoring system of the available kinetic energy in a grid level that can be released to improve the settling frequency. Thus, it has a high cost. In [11], an improved method of a DFIG based on the over-speed and de-loaded curve was introduced to reduce the ROCOF. A synergistic control strategy was proposed in [12] considering mechanical stresses on the equipment associated with the pitch angle controller and its slow response speed. When a disturbance occurs, the speed and pitch angle controllers cooperate to provide the optimum operation by shifting the operating point of the wind turbine to a higher power extraction point and releasing the reserved power. In [13], a switching angle controller and automatic generation controller were introduced for a DFIG to support the system frequency. This method aims to regulate the output active power of the DFIG by controlling the angle between the terminal voltage and the internal voltage of the DFIG, which is called the virtual rotor angle. This method is complicated. In [14] and [15], the system frequency was supported by continuously adjusting the droop parameter according to the wind speed. In [16], an optimized power point tracking strategy was proposed for primary frequency regulation. A simplified model of a DFIG-based wind turbine was used to evaluate the proposed method. In [17], a bang-bang phase angle controller (BPAC) was presented to regulate the system frequency by controlling the phase angle obtained with a phase-locked loop directly. The output of BPAC is fed into the pitch angle controller. In [18], the DFIG and energy storage (ES) were combined together for system frequency support. However, this technique needs more investigation on how can employ the ES to realize the optimal operation of wind turbine generators. In [19], the rotating mass connected to the DFIG shaft or a super-capacitor connected to the DC-link of a DFIG-converter was used as the virtual inertia source. Although the results proved the effectiveness of the super-capacitor for enhancing the system frequency, this method requires additional components which makes it costly.

An artificial neural network (ANN) was introduced in [20] to find the optimum gain of the droop controller according to the wind speed, and load disturbance. The results proved that the proposed method has the best performance compared to the fixed-gain controller. In [21], a coordinated control parameter setting method for wind farms by an optimization model was presented. Although it has a good performance for improving the system frequency, it is complicated. In [22], the system frequency was improved based on the dynamic deloading of DFIG. The operating costs and prediction error of wind power were taken into consideration. In [23], a torque limit-based inertial control scheme of a DFIG was presented to system frequency support. At disturbances, the DFIG output power is increased up to the torque limit in a stable operating range. A comprehensive overview of the previous frequency control techniques and the proposed method is listed in Appendix.

Some of the previous methods are complicated [13], [20], [21], [24]. The cost is high in [7], [10], and [19], and the response is slow in [4] and [6]. To address the previous issues, a fast and improved method is introduced for better frequency regulation of DFIG- based wind turbines. The main contributions of this work can be summarized in the following points:

- A supplemental control, washout filter, is added to the primary frequency control of a DFIG-based wind turbine for system frequency regulation.
- The philosophy and settings of the improved method are simple and easy to be implemented in practice compared to the previous studies.
- A recent optimization technique, Mayfly Algorithm (MA), is applied for system frequency support.
- The impact of the washout filter's parameters on the system frequency response and stability is investigated.

The rest of the paper is organized as follows. The system frequency support method is presented in Section II. Mayfly Algorithm is described in Section III. Simulation results and discussions are carried out in Section IV. The conclusion is drawn in Section V.

II. SYSTEM FREQUENCY SUPPORT METHOD

A. TRADITIONAL METHOD

It comprises frequency control support, inertia emulation control, and active power control, as shown in Fig.1.

In frequency control support, the difference between the reference and measured frequencies, Δf, is applied to the gain K_f, where the output of frequency control support is proportional to the Δf. In inertia emulation control, the measured frequency is fed into the derivative block. Then, the output is multiplied by the gain K_{in}. In the active power control, the

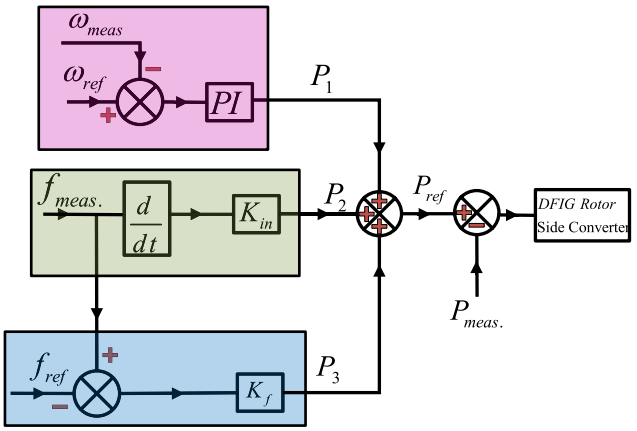

FIGURE 1. Scheme of the traditional method. Lower branch: frequency control support. Middle branch: inertia emulation control. Upper branch: active power control [25].

difference between the reference and measured rotor speeds is fed to the PI controller [25], [26]. The output of the traditional method is called reference active power (P_{ref}). In the steady-state condition, P_{ref} equals the output of the PI controller (P_1), where the output of both frequency control support (P_3) and inertia emulation control (P_2) equals zero. During changing the load, both the P_2 and P_3 don't equal zero. Consequently, the reference active power is increased. That is to say, the traditional method regulates the reference active power of a DFIG rotor side converter which in turn controls the rotor voltage of a DFIG. Thus, the reserved active power of a DFIG is quickly increased (decreased) and thus the frequency deviation decreases.

B. IMPROVED METHOD

The main objective is to increase the reference active power of a DFIG, leading to less frequency deviation. When the output power increases (decreases), both the rotor speed and electrical frequency decrease (increase). The electrical frequency is proportional to the rotor speed. Thus, any change in the power causes a change in both the rotor speed and system frequency. The relation between the change in the active power and the change in the frequency can be written as:

$$\Delta f + m_p \Delta P = 0 \tag{1}$$

where m_p is a constant value, f is the electrical frequency according to the rotor speed, and P is the output active power. By taking the derivative of Eq. (1) with respect to time, the following equation can be obtained:

$$\frac{d}{dt}\Delta f + m_p \frac{d}{dt}\Delta P = 0 \tag{2}$$

It is clear that the derivative of the above equation is equal to zero in the steady-state condition, where the Δf and ΔP are constants. Another term, $n_p\ \Delta f$, is added to guarantee less frequency deviation as follows:

$$\frac{d}{dt}\Delta f + m_p \frac{d}{dt}\Delta P + n_p \Delta f = 0 \tag{3}$$

where n_P is a constant value. by applying laplace transform to equation (3), the following equation is obtained:

$$s\Delta f(s) + m_p s\Delta P(s) + n_p \Delta f(s) = 0 \tag{4}$$

$$\frac{\Delta P(s)}{\Delta f(s)} = -\frac{(s + n_p)}{m_p s} \tag{5}$$

It can be noted that Eq. (5) represents the transfer function of the washout filter which is a first-order high pass filter. The main objective of the washout filter is to pass the transient signals (during load variation), whereas it rejects the steady-state signals (DC component). Fig.2 shows the scheme of the improved method.

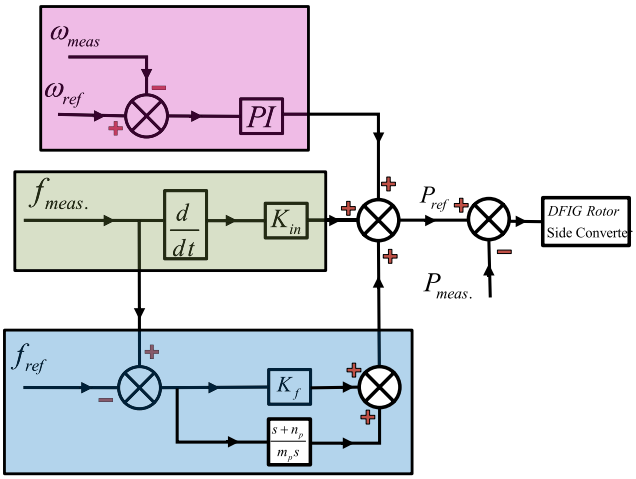

FIGURE 2. Scheme of the improved method. Lower branch: improved frequency control support. Middle branch: inertia emulation control. Upper branch: active power control.

III. MAYFLY ALGORITHM

In [27], the authors have presented a new optimization algorithm called Mayfly Algorithm (MA). The MA includes the major advantages of evolutionary algorithms and swarm intelligence. Thereby, it has a higher probability of discovering a global optimum compared to the most popular metaheuristic optimization techniques [27]. In this study, the MA is used to obtain the optimal parameters of the washout filter (m_p and n_p) which achieve the lowest frequency deviation as well as improving the system stability.

The integral of squared error is used as a fitness function and can be written as:

$$Fitness\ \text{Function} = \int_0^{tsim} (\Delta f)^2\, dt \tag{6}$$

where t_{sim} represents the simulation time, and Δf represents the frequency deviation.

The power system model and fitness function are built in MATLAB/SIMULINK, whereas the MA code is executed in MATLAB/m.file. The value of the fitness function is exported to the MA code via workspace. The process of linking the MA code with the power system model for finding the optimum

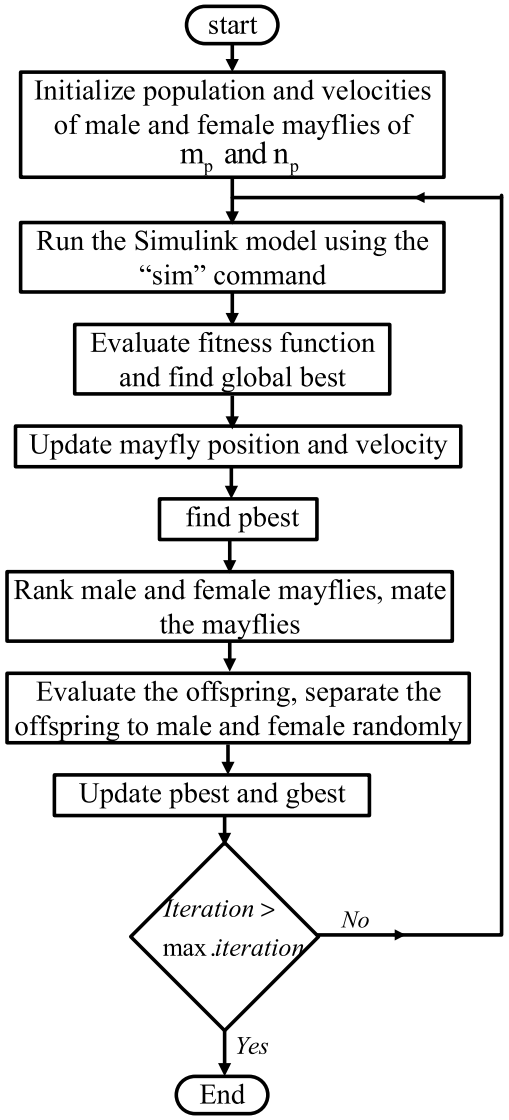

FIGURE 3. Flow chart of linking the MA with power system model for identifying the optimum values of m_p and n_p.

values of m_p and n_p is shown in Fig.3. The MA is used as an offline algorithm to design the washout filter before its adding to the real power system.

The parameters of the MA technique and the optimal values of the washout filter (m_p and n_p) are given in Table 1.

IV. SIMULATION RESULTS AND DISCUSSIONS

A. SYSTEM CONFIGURATION

In this work, the studied system consists of two synchronous generators with 675 MW for each one, DFIG wind turbines with 150 MW, and three loads that are connected in parallel across 230 kV, as shown in Fig.4. Synchronous generator includes automatic generation control (AGC). The 150 MW wind turbines are an aggregated model of 100 DFIG units, where each unit has a power rating of 1.5 MW [7]. Load 1 absorbs 1278 MW and 50 MVAR. Load 2 absorbs

TABLE 1. Specification of the MA technique.

Parameter	Value
Population size (n_{pop})	20
Lower bound	1e-5
Upper bound	0.9
Inertia weight (g)	0.8
Inertia weight damping ratio (g_{damp})	0.93
Personal learning coefficient (a_1)	1.0
Global learning coefficient (a_2 and a_3)	1.5
Distance sight coefficient (β)	2.0
Nuptial dance	5.0
Random flight	1.0
Damping ratio 1 (dance damp)	0.8
Damping ratio 2 (flight damp)	0.99
Number of offsprings	20
Mutation rate	0.01
Number of mutants	round ($0.05*n_{pop}$)
m_p	0.0544
n_p	0.0258
Max. iteration	25

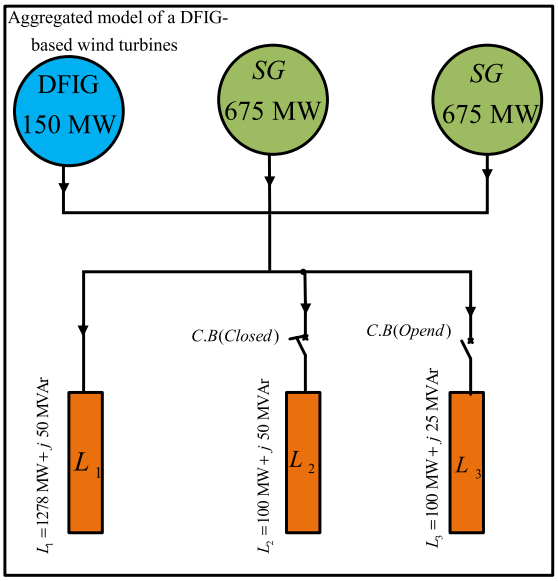

FIGURE 4. Simplified model of the study system.

100 MW and 50 MVAR. Load 3 absorbs 100 MW and 25 MVAR. The studied system is established in MATLAB/SIMULINK software to evaluate the performance of the improved method.

B. THE IMPACT OF THE WASHOUT FILTER'S PARAMETER (n_p) ON THE SYSTEM FREQUENCY RESPONSE AND STABILITY

In this subsection, the effect of n_p on the system frequency response and stability is investigated, where the simulation is carried out at different values of n_p as shown in Fig.5. The initial load connected to the system is L_1 ($P_1 + j\,Q_1$). Then, a second load L_2 ($P_2 + j\,Q_2$) is connected at t = 50 sec. The value of $m_p = 0.02$ in all studied cases. The frequency

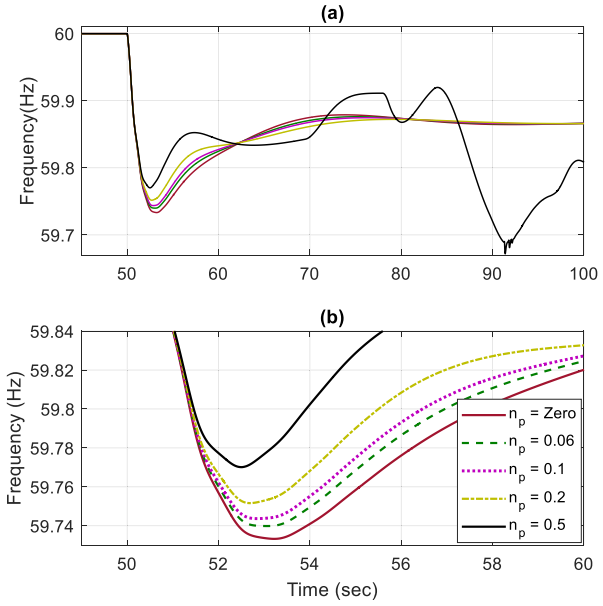

FIGURE 5. Frequency system response at different values of n_p.

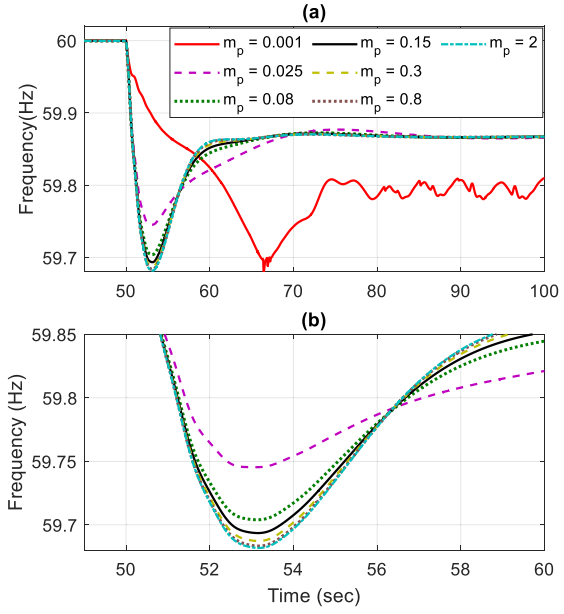

FIGURE 6. Frequency system response at different values of m_p.

deviation (Δf = 60–lowest frequency drop) at different values of n_p is listed in Table 2.

The following notes can be drawn from Fig.5:

1- The lowest frequency drop is equal to 59.73 Hz, 59.74 Hz, 59.744 Hz, 59.75 Hz, and 59.77 Hz for n_p = zero, n_p = 0.06, n_p = 0.1, n_p = 0.2, and n_p = 0.5, respectively. The least value of frequency deviation achieves with a higher value of n_p.

2- The system is more stable by decreasing the value of n_p where the system is unstable when n_p equals 0.5.

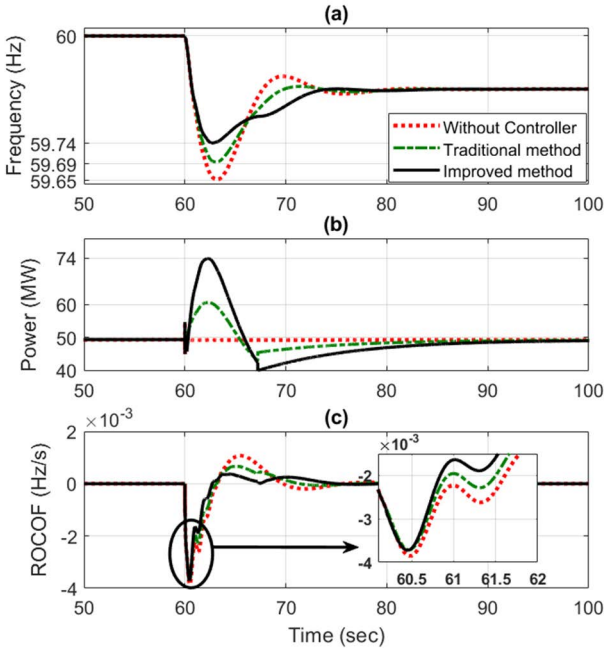

FIGURE 7. Dynamic response in case of increasing the load: (a) Frequency, (b) Output active power, and (c) ROCOF.

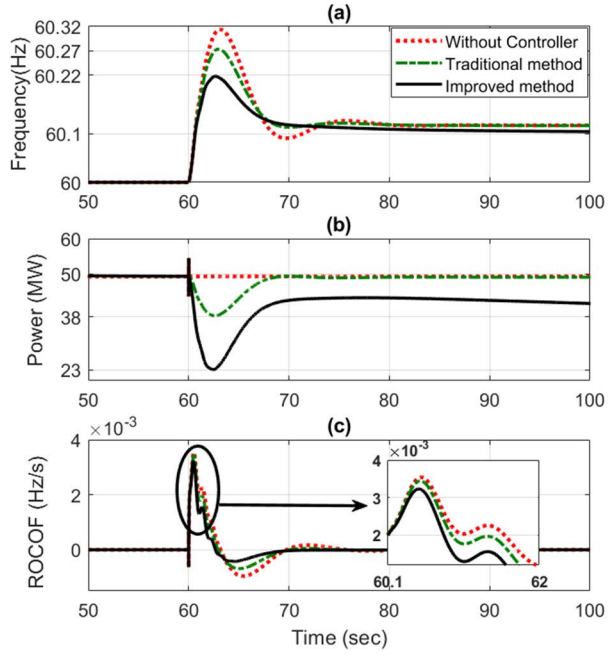

FIGURE 8. Dynamic response in case of reducing the load: (a) Frequency, (b) Output active power, and (c) ROCOF.

C. THE IMPACT OF THE WASHOUT FILTER'S PARAMETER (m_p) ON THE SYSTEM FREQUENCY RESPONSE AND STABILITY

The simulation is repeated again at different values of m_p in order to examine its influence on the system frequency and stability as shown in Fig. 6. All cases are set up for n_p = 0.05, and the initial load is L_1 (P_1+ j Q_1). At t = 50 sec,

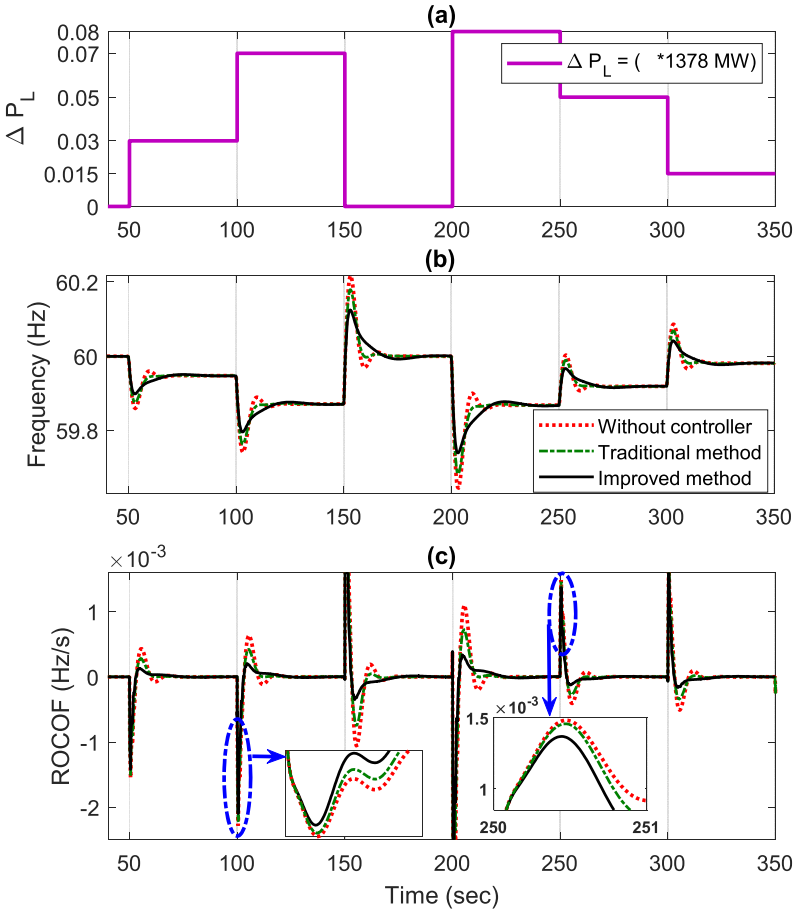

FIGURE 9. Dynamic response of multi-step load perturbation: (a) ΔP_L, (b) Frequency, and (c) ROCOF.

TABLE 2. Frequency deviation corresponding to the different values of n_p.

n_p	Lowest frequency drop	Frequency deviation
0	59.73	0.27
0.06	59.74	0.26
0.1	59.744	0.256
0.2	59.75	0.25
0.5	59.77	0.23

TABLE 3. Frequency deviation corresponding to the different values of m_p.

m_p	Lowest frequency drop	Frequency deviation
0.025	59.748	0.252
0.08	59.709	0.291
0.15	59.695	0.305
0.3	59.688	0.312
0.8	59.686	0.314
2	59.685	0.315

a second load L_2 (P_2+ j Q_2) is connected to the system. Table 3 shows the lowest frequency drop corresponding to the different values of m_p.

The following notes can be extracted from Fig.6:

1- The lowest frequency drop equals 59.748 Hz, 59.709 Hz, 59.695 Hz, 59.688 Hz, 59.686 Hz, and 59.685 Hz for $m_p = 0.025$, $m_p = 0.08$, $m_p = 0.15$, $m_p = 0.3$, $m_p = 0.8$, and $m_p = 2$, respectively. That is to say, the higher the mp, the higher the frequency deviation.

2- The system lacks stability with a lower value of mp, where there is an oscillation when $m_p = 0.001$.

From Figs. 5 and 6, the values of mp and np have a detrimental effect on the system stability. Thus, the MA is used to determine the optimal values of np and mp which achieve the lowest deviation with keeping the system stable.

D. THE IMPACT OF INCREASING THE LOAD ON THE SYSTEM DYNAMIC RESPONSE

Initially, both L_1 and L_2 are connected to the system. Then, an additional load (L_3) is connected via the circuit breaker at t = 60 sec. The optimal parameters of the washout filter are listed in Table 1. Fig.7 shows the system dynamic response of frequency (Hz), active power (MW), and ROCOF (Hz/s) with the traditional method, improved method, and without a controller.

TABLE 4. A comprehensive overview of the previous frequency control techniques and the proposed method.

Method in Ref.	The used technique	Advantages	Disadvantages
[4]	• A supplementary control loop was added to a DFIG controller. • It includes a derivative block, first-order filter block, and again block	• Simple design	• Low-frequency nadir
[5]	• A non-standard inertial response method was proposed to support the system frequency, where the inertia constant is estimated according to the rotor speed	• Moderate response	• Requires some information to calculate the inertia constant corresponding to the rotor speed.
[28],[29]	• Constant fast power reserve	• Fast response	• Unstable operation
[6]	• Droop control using linear adjustment of power output.	• Simple design	• Low-frequency nadir • Second frequency dip
[9]	• Droop control using variable droop control gain.	• Improved frequency nadir	• Slow response • Complex design
[30],[11],[12]	• Deloading control using speed control and pitch angle control.	• Stable operation	• Slow response • Complex design
[16]	• A virtual inertia controller version of the optimized power point tracking method.	• Smoother output power	• Slow response • Low-frequency nadir
[13]	• Switching angle controller (SAC) and automatic generation control (AGC).	• Fast response	• Complex design • Doesn't respond to small disturbances
[17]	• Bang-bang phase angle controller (BPAC)	• Stable operation	• Complex design • Slow response
[7]	• Flywheel energy storage system	• Moderate frequency nadir	• Highly cost
[19]	• A super-capacitor connected to the DC-link of a DFIG-converter.	• Fast response	• Highly cost
[20]	• Artificial neural network (ANN)-based supplementary frequency controller.	• Fast response	• Complex design
[31]	• The second derivative of the system frequency-based strategy	• Moderate frequency nadir	• Complex design
[21]	• A coordinated control parameter setting method of DFIG wind farms	• Improved system small-signal stability	• Complex design
[22]	• Dynamic deloading control technique	• Stable operation	• Complex design • Slow response
Proposed method	• Supplemental control (washout filter) for system frequency support of DFIG-based wind turbines.	• Fast response and easy to be implemented	• Parameters of supplementary control have to be selected carefully

The following conclusions can be extracted from Fig.7:

1- The lowest frequency drop is achieved by the improved method as shown in Fig.7(a), where the frequency drops to 59.74 Hz. Whereas the frequency drops to 59.69 Hz with the traditional method and 59.65 Hz without controller.

2- A higher reserved power is provided by the improved method (74–50 = 24 MW) compared to the traditional method (60–50 = 10 MW) as shown in Fig.7(b).

3- The improved method achieves the lowest values for overshoot, and undershoot compared to the traditional method as shown in Fig.7(c).

E. THE IMPACT OF REDUCING THE LOAD ON THE SYSTEM DYNAMIC RESPONSE

Initially, both L_1 and L_2 are connected to the system. Then, L_2 is removed via the circuit breaker at t = 60 sec. The system dynamic response with the improved method, traditional method, and without controller are plotted in Fig.8.

The following observations are derived from Fig.8:

1- Fig.8(a) shows that the frequency overshoot reaches 60.32 Hz, 60.27 Hz, and 60.22 Hz for controller OFF, traditional controller, and improved controller, respectively.
2- More reserved active power is given by the improved method (50-23 = 27 MW) compared to the traditional method (50–38 = 12 MW), trying to support the system frequency against reducing the load as shown in Fig.8 (b).
3- The improved method presents a smaller ROCOF compared to the traditional method as shown in Fig.8(c).
4- These results prove that the improved method can enhance the system frequency effectively, where it provides better performance in comparison with the traditional method.

F. THE IMPACT OF MULTI-STEP LOAD PERTURBATION ON THE SYSTEM DYNAMIC RESPONSE

The main objective of this scenario is to confirm conclusively the performance of the improved method when a series load disturbance is applied to the studied system. Fig. 9(a) shows the percent of a series load, where ΔP_L ranges between zero to 8 % of the initial load (L_1 and L_2). The following notes can be concluded from Fig. 9:

1- The improved method can achieve overshoot, oscillation, and undershoot values less than those that are achieved by the traditional method.
2- The improved method has robust performance in facing sudden load changes compared to the traditional method.

V. CONCLUSION

In this paper, the washout filter has been added to the primary frequency control of a DFIG-based wind turbine for frequency stability enhancement. The impact of the washout filter's parameters (m_p and n_p) on the system stability and frequency deviation has been investigated. The simulation results have revealed that: 1) the value of m_p is proportional to both the stability and frequency deviation. 2) the value of n_p is inversely proportional to both the stability and frequency deviation. Thus, the washout filter's parameters have been identified based on the MA technique to maintain the system stable and reduce the frequency deviation at the same time. Also, the simulation outcomes have confirmed that the improved method has the best performance compared to the traditional method, where the lowest frequency deviation has been achieved by the improved method under different load disturbances.

APPENDIX

See Table 4.

ACKNOWLEDGMENT

This project has received funding from the European Union's Horizon 2020 research and innovation programme under Marie Skłodowska-Curie grant agreement No. 801342 (Tecniospring INDUSTRY) and the Government of Catalonia's Agency for Business Competitiveness (ACCIÓ).

REFERENCES

[1] X. Yingcheng and T. Nengling, "Review of contribution to frequency control through variable speed wind turbine," *Renew. Energy*, vol. 36, no. 6, pp. 1671–1677, 2011.
[2] A. B. Attya, J. L. Dominguez-Garcia, and O. Anaya-Lara, "A review on frequency support provision by wind power plants: Current and future challenges," *Renew. Sustain. Energy Rev.*, vol. 81, pp. 2071–2087, Jan. 2018.
[3] A. Ostadi, A. Yazdani, and R. K. Varma, "Modeling and stability analysis of a DFIG-based wind-power generator interfaced with a series-compensated line," *IEEE Trans. Power Del.*, vol. 24, no. 3, pp. 1504–1514, Jul. 2009.
[4] J. Ekanayake and N. Jenkins, "Comparison of the response of doubly fed and fixed-speed induction generator wind turbines to changes in network frequency," *IEEE Trans. Energy Convers.*, vol. 19, no. 4, pp. 800–802, Dec. 2004.
[5] L. Wu and D. G. Infield, "Towards an assessment of power system frequency support from wind plant—Modeling aggregate inertial response," *IEEE Trans. Power Syst.*, vol. 28, no. 3, pp. 2283–2291, Aug. 2013.
[6] W. Yao and K. Y. Lee, "A control configuration of wind farm for load-following and frequency support by considering the inertia issue," in *Proc. IEEE Power Energy Soc. Gen. Meeting*, Jul. 2011, pp. 1–6.
[7] F. Díaz-González, M. Hau, A. Sumper, and O. Gomis-Bellmunt, "Coordinated operation of wind turbines and flywheel storage for primary frequency control support," *Int. J. Electr. Power Energy Syst.*, vol. 68, pp. 313–326, Jun. 2015.
[8] K. E. Okedu, "A variable speed wind turbine flywheel based coordinated control system for enhancing grid frequency dynamics," *Int. J. Smart Grid*, vol. 2, no. 2, pp. 123–134, Nov. 2018.
[9] Y.-L. Hu and Y.-K. Wu, "Approximation to frequency control capability of a DFIG-based wind farm using a simple linear gain droop control," *IEEE Trans. Ind. Appl.*, vol. 55, no. 3, pp. 2300–2309, May 2019.
[10] J. I. Yoo, Y. C. Kang, E. Muljadi, K.-H. Kim, and J.-W. Park, "Frequency stability support of a DFIG to improve the settling frequency," *IEEE Access*, vol. 8, pp. 22473–22482, 2020.
[11] Y. Xu, H. Wang, and D. Yang, "An enhanced frequency response strategy of a DFIG based on over-speed de-loaded curve," *Appl. Sci.*, vol. 11, no. 19, p. 9324, Oct. 2021.
[12] R. Prasad and N. P. Padhy, "Synergistic frequency regulation control mechanism for DFIG wind turbines with optimal pitch dynamics," *IEEE Trans. Power Syst.*, vol. 35, no. 4, pp. 3181–3191, Jul. 2020.
[13] Y. Liu, L. Jiang, Q. H. Wu, and X. Zhou, "Frequency control of DFIG-based wind power penetrated power systems using switching angle controller and AGC," *IEEE Trans. Power Syst.*, vol. 32, no. 2, pp. 1553–1567, Mar. 2017.
[14] K. V. Vidyanandan and N. Senroy, "Primary frequency regulation by deloaded wind turbines using variable droop," *IEEE Trans. Power Syst.*, vol. 28, no. 2, pp. 837–846, May 2013.
[15] J. Zhao, X. Lyu, Y. Fu, X. Hu, and F. Li, "Coordinated microgrid frequency regulation based on DFIG variable coefficient using virtual inertia and primary frequency control," *IEEE Trans. Energy Convers.*, vol. 31, no. 3, pp. 833–845, Sep. 2016.
[16] D. Ochoa and S. Martinez, "Fast-frequency response provided by DFIG-wind turbines and its impact on the grid," *IEEE Trans. Power Syst.*, vol. 32, no. 5, pp. 4002–4011, Sep. 2017.
[17] Y. Liu, L. Jiang, J. S. Smith, and Q. H. Wu, "Primary frequency control of DFIG-WTs using bang-bang phase angle controller," *IET Gener., Transmiss. Distrib.*, vol. 12, no. 11, pp. 2670–2678, Jun. 2018.
[18] L. Miao, J. Wen, H. Xie, C. Yue, and W. J. Lee, "Coordinated control strategy of wind turbine generator and energy storage equipment for frequency support," *IEEE Trans. Ind. Appl.*, vol. 51, no. 4, pp. 2732–2742, Jul. 2015.
[19] M. F. M. Arani and E. F. El-Saadany, "Implementing virtual inertia in DFIG-based wind power generation," *IEEE Trans. Power Syst.*, vol. 28, no. 2, pp. 1373–1384, May 2013.
[20] T.-H. Chien, Y.-C. Huang, and Y.-Y. Hsu, "Neural network-based supplementary frequency controller for a DFIG wind farm," *Energies*, vol. 13, no. 20, p. 5320, Oct. 2020.
[21] J. Liu, Z. Yang, J. Yu, J. Huang, and W. Li, "Coordinated control parameter setting of DFIG wind farms with virtual inertia control," *Int. J. Electr. Power Energy Syst.*, vol. 122, Nov. 2020, Art. no. 106167.

[22] J. Ouyang, M. Pang, M. Li, D. Zheng, T. Tang, and W. Wang, "Frequency control method based on the dynamic deloading of DFIGs for power systems with high-proportion wind energy," *Int. J. Electr. Power Energy Syst.*, vol. 128, Jun. 2021, Art. no. 106764.
[23] M. Kang, K. Kim, E. Muljadi, J. W. Park, and Y. C. Kang, "Frequency control support of a doubly-fed induction generator based on the torque limit," *IEEE Trans. Power Syst.*, vol. 31, no. 6, pp. 4575–4583, Nov. 2016.
[24] A. H. A. Elkasem, M. Khamies, G. Magdy, I. B. M. Taha, and S. Kamel, "Frequency stability of AC/DC interconnected power systems with wind energy using arithmetic optimization algorithm-based fuzzy-PID controller," *Sustainability*, vol. 13, no. 21, p. 12095, Nov. 2021.
[25] J. Morren, S. W. H. de Haan, W. L. Kling, and J. A. Ferreira, "Wind turbines emulating inertia and supporting primary frequency control," *IEEE Trans. Power Syst.*, vol. 21, no. 1, pp. 433–434, Feb. 2006.
[26] R. Chen, W. Wu, H. Sun, Y. Hu, and B. Zhang, "Supplemental control for enhancing primary frequency response of DFIG-based wind farm considering security of wind turbines," in *Proc. IEEE PES Gen. Meeting|Conf. Expo.*, Jul. 2014, pp. 1–5.
[27] K. Zervoudakis and S. Tsafarakis, "A mayfly optimization algorithm," *Comput. Ind. Eng.*, vol. 145, Jul. 2020, Art. no. 106559.
[28] S. Wachtel and A. Beekmann, "Contribution of wind energy converters with inertia emulation to frequency control and frequency stability in power systems," Energynautics GmbH, Langen, Germany, Tech. Rep., 2009.
[29] A. D. Hansen, M. Altin, I. D. Margaris, F. Iov, and G. C. Tarnowski, "Analysis of the short-term overproduction capability of variable speed wind turbines," *Renew. Energy*, vol. 68, pp. 326–336, Aug. 2014.
[30] L. M. Castro, C. R. Fuerte-Esquivel, and J. H. Tovar-Hernandez, "Solution of power flow with automatic load-frequency control devices including wind farms," *IEEE Trans. Power Syst.*, vol. 27, no. 4, pp. 2186–2195, Nov. 2012.
[31] M. V. Kazemi, S. J. Sadati, and S. A. Gholamian, "Adaptive frequency control support of a DFIG based on second-order derivative controller using data-driven method," *Int. Trans. Elect. Energy Syst.*, vol. 30, no. 7, 2020, Art. no. e12424.

MOHAMED ABDEEN received the B.Sc. and M.Sc. degrees in electrical engineering from Al-Azhar University, Cairo, Egypt, in 2011 and 2016, respectively, and the Ph.D. degree from Chongqing University, Chongqing, China, in 2020. He is currently an Assistant Professor with the Department of Electrical Engineering, Al-Azhar University. His research interests include power system stability, optimization, and control.

MUHAMMAD SAYYED received the B.S. degree from the Department of Electrical Engineering, Faculty of Engineering, Al-Azhar University, in 2020. He is currently working as an Electrical Design and Simulation Engineer with Future Technologies Ltd. His research interests include the frequency stability of power systems, renewable energy systems, and power system protection.

JOSÉ LUIS DOMÍNGUEZ-GARCÍA (Senior Member, IEEE) received the B.S. and M.S. degrees in industrial engineering in 2009 and the Ph.D. degree in electrical engineering in 2013. He was a Visiting Researcher with the Institute of Energy, Cardiff University, in 2011; the University of Strathclyde, Glasgow, in 2016; and Huddersfield University, U.K., in 2018. In 2010, he joined IREC, as a Researcher, where he is currently acts as the Head of the Power Systems Group. He is also the General Coordinator of the H2020 COREWIND and INCITE H2020 MSCA ITN projects as well as the WP leader of others. His work deals with the grid integration of renewable energy sources, smart grids, and microgrids.

SALAH KAMEL received the international Ph.D. degree from the University of Jaén, Spain (Main), and Aalborg University, Denmark (Host), in January 2014. He is currently an Associate Professor with the Department of Electrical Engineering, Aswan University. His research activities include power system analysis and optimization, smart grid, and renewable energy systems.